



**Reactions of Tungsten Propargyl and Allenyl Complexes with Hydrido
Triosmium Cluster: Molecular and Crystal Structure of
Cp(CO)₂[P(OMe)₃]W(μ, η^1, η^2 -CH₂CH=CH)Os₃(CO)₁₀H and
H₂(CH₂CH=CH)₂Os₆(CO)₂₀**

Tian-Wen Tseng (曾添文), Ming-Chou Chen (陳銘洲), Rai-Shing Keng (耿瑞星),
Ying-Chih Lin* (林英智), Gene-Hsiang Lee (李錦祥) and Yu Wang (王瑜)

Department of Chemistry, National Taiwan University, Taipei, Taiwan 10764, Republic of China

Reactions of H₂Os₃(CO)₁₀, **3**, with the monophosphite-substituted and non-substituted tungsten propargyl and allenyl carbonyl complexes Cp(CO)₂LWCH₂C≡CH (**1a**, L = CO; **1b**, L = P(OMe)₃) and Cp(CO)₂LWCH=C=CH₂ (**2a**, L = CO; **2b**, L = P(OMe)₃) were investigated. In the reaction of **1b** with **3**, a tetranuclear complex **4b** is obtained. The molecules of **4b** crystallize as Cp(CO)₂[P(OMe)₃]W(μ, η^1, η^2 -CH₂CH=CH)(μ -H)Os₃(CO)₁₀ in space group P $\bar{1}$ with $a = 9.490(4)$, $b = 13.072(7)$, $c = 13.770(9)$ Å, $\alpha = 91.89(5)$, $\beta = 106.71(5)$, $\gamma = 104.07(4)^\circ$, $V = 1577(2)$ Å³, $Z = 2$. In the reaction of **2a** with **3**, from the reaction mixture exposed to air followed by workup using silica-gel packed column chromatography, a complex consisting of two triosmium clusters bridged by a hexadiene ligand from the coupling of allenyl ligand was obtained. The molecules of the hexanuclear complex crystallize as [CH₂CH=CH]₂(μ -H)₂Os₆(CO)₂₀ in space group P2₁/c with $a = 14.448(7)$, $b = 13.689(4)$, $c = 19.224(4)$ Å, $\beta = 107.14(3)^\circ$, $V = 3633(2)$ Å³, $Z = 4$.

INTRODUCTION

The self addition of alkenes, dienes or alkynes to form dimers, trimers and low polymers is termed oligomerization. The mechanisms are essentially the same as for polymerization except that chain termination occurs much more frequently. Both dimerization of ethene, propene and higher olefins and their codimerization have been achieved with many catalytic systems. Some are typical Ziegler systems, for instance, cobalt(II) acetylacetonate triethylaluminum; in others the active species is formed by oxidative addition of HCl to Rh(I). The exact nature of the active species has generally not been elucidated in the various recipes for catalytic systems. By far the most active dimerization catalysts for ethene and propene are based on nickel compounds, and in particular on π -allylnickel halides.¹² We recently reported transformation of a tungsten propargyl complex Cp(CO)₃WCH₂C≡CH, **1a**, to the corresponding allenyl complex Cp(CO)₃WCH=C=CH₂, **2a**.³ Then, dimerization of the coordinated allenyl ligand to 1,5-hexadiene was observed in the reaction of H₂Os₃(CO)₁₀, **3**, with **2a**.⁴ The transformation of **1a** to **2a**

is unidirectional: no propargyl complex was detected in a solution of allenyl complex by a spectral method. The existence of these isomeric metal complexes provides a unique system for the exploration of chemical reactivities of organic propargyl/allenyl ligands which coordinate to tungsten metal in varied fashion. For example, in the reactions of amine with complexes **1a** and **2a**, two types of regioselective C-C bond formation have been observed;⁵ although C-C bond formation takes place at the β -carbon of the propargyl C₃ unit, C-C bond formation of a similar type occurs at the α -carbon of the allenyl ligand. In the reaction of **2a** with **3**, the mechanism for the dimerization of the allenyl ligands to hexadiene and the transfer of this ligand to the triosmium cluster, was unclear. A dimerization of similar type was observed in a tetrakis(allyl)molybdenum dimer containing a quadruple metal-metal bond.⁶ In order to understand better the chemical reactivities of the propargyl and the allenyl ligands and the mechanism of the dimerization, we carried out reactions of the non-substituted and substituted tungsten complexes with metal hydrides. We report here our results on the reactions of H₂Os₃(CO)₁₀ with tungsten propargyl and allenyl com-

Dedicated to Professor Sheng-Lieh Liu (劉盛烈) on the occasion of his eightieth birthday.



plexes and their phosphite substituted analogues.

EXPERIMENTAL SECTION

General Procedures

All manipulations were performed under dinitrogen using a vacuum line, drybox and standard Schlenk techniques. NMR spectra were recorded on a Bruker AM-300WB spectrometer and are reported in units of parts per million with residual protons in the solvent as an internal standard (C_6D_6 , δ 7.15). IR spectra were recorded on Perkin-Elmer 983 instrument and wavenumbers (cm^{-1}) were measured relative to a polystyrene standard. Electron-impact mass spectra were determined with a Finnigan TSQ-46C spectrometer. Diethyl ether was distilled from CaH_2 and stored over molecular sieves prior to use. Benzene and CH_2Cl_2 were distilled from $LiAlH_4$ and CaH_2 , respectively. THF was distilled from sodium-benzophenone. All other solvents and reagents were of reagent grade and used without further purification. $W(CO)_6$ and $Os_3(CO)_{12}$ (Strem), propargyl bromide, allyl bromide (Merck, distilled in small quantity before use) were obtained commercially. Complexes $[CpW(CO)_3]_2$,⁷ $[CpW(CO)_2P(OMe)_3]_2Hg$,⁸ and $H_2Os_3(CO)_{10}$ ⁹ were prepared according to the literature methods. The tungsten complex $CpW(CO)_3CH_2C\equiv CH$, and its trimethylphosphite substituted analogue¹⁰ were prepared from the tungsten anions $CpW(CO)_2L^-$ ($L = CO$ and $L = P(OMe)_3$) which were prepared from the Na/Hg reduction¹¹ of $[CpW(CO)_3]_2$ and $[CpW(CO)_2WP(OMe)_3]_2Hg$, respectively. The allenyl complex $Cp(CO)_3WCH=C=CH_2$, and its phosphite substituted analogue were prepared from the corresponding propargyl complexes.⁴

Reaction of $Cp(CO)_3W(CH_2C\equiv CH)$ (1a) with $H_2Os_3(CO)_{10}$

A solution of $H_2Os_3(CO)_{10}$ (210 mg, 0.25 mmol) in C_6H_6 (5 mL) was added slowly at room temperature to a solution of **1a** (74 mg, 0.20 mmol) in C_6H_6 (2.5 mL). The solution was stirred for 1.5 h, then the volume of the solvent was reduced under vacuum to cause precipitation and the solid was separated from the mixture and then redissolved in hexane to give a yellow solution. As solid residue was removed by filtration. Removal of the solvent produced $Cp(CO)_3W(\mu,\eta^1,\eta^2-CH_2CH=CH)(\mu-H)Os_3(CO)_{10}$, **4a** (83 mg, 0.068 mmol) as a red powder in 34% yield based on **W**. Spectral data for **4a**: 1H NMR (C_6D_6) 6.43 (*dd*, $J_{H-H} = 14.7, 1.7$ Hz, =CH), 5.63 (*dd*, $J_{H-H} = 14.7, 8.0$ Hz, =CH), 4.30 (*s*, Cp); 2.02 (*d*, $J_{H-H} = 8.0$ Hz, CH_2); -17.8 (*d*, $J_{H-H} = 1.7$ Hz,

Os-H-Os). ^{13}C NMR data are unavailable because the complex decomposed during data acquisition. When the reaction was carried out in small quantity with excess **3** and monitored by NMR spectra, a hydrogenation product $Cp(CO)_3W(CH_2CH=CH_2)$ (**5a**) and $(\mu,\eta^1,\eta^2-CH_3CH=CH)(\mu-H)Os_3(CO)_{10}$ (**6**) was observed in the spectra. Complex **5a** was also prepared from the reaction of $Cp(CO)_3W$ with allylic bromide. Spectral data for **5a**: IR (CH_3CN) 2009 (*s*), 1907 (*vs*, ν_{CO}), 1610 (*m*, $\nu_{C=C}$) cm^{-1} ; 1H NMR (C_6D_6) 6.10 (*m*, $J_{H-H} = 16.6, 9.8, 8.4$ Hz, =CH), 4.75 (*m*, $J_{H-H} = 16.6, 2.1, 1.1$ Hz, =CH), 4.58 (*dd*, $J_{H-H} = 9.8, 2.1$ Hz, =CH), 4.43 (*s*, Cp), 2.29 (*dd*, $J_{H-H} = 8.4, 1.1$, CH_2); ^{13}C NMR (C_6D_6) 229.4, 217.6 (CO), 146.2 (=C β), 107.5 (=C γ), 92.4 (*s*, Cp), -6.4 (CH_2); Anal. Calcd for $C_{11}H_{10}O_3W$: C, 35.32; H, 2.69. Found: C, 35.14, H, 2.33. Spectral data of **6** are given below.

Reaction of $Cp(CO)_3W(CH=C=CH_2)$ (2a) with **3**

A solution of $H_2Os_3(CO)_{10}$ (85 mg, 0.10 mmol) in C_6D_6 (0.5 mL) was added slowly at room temperature to a solution of **2a** (40 mg, 0.11 mmol) in C_6D_6 (1 mL). The reaction was monitored by NMR spectroscopy. An intermediate which exhibited resonances at δ 6.10, 4.75, 4.60, 4.41 and 2.30 with intensity ratio 1:1:1:5:3 in the 1H NMR spectra was observed in about 60% NMR yield. Coupling parameters 17.2, 12.0 and 7.9 Hz were observed between the resonance at 6.10 ppm and the resonances at 4.75, 4.60 and 2.30, respectively. The solvent was reduced in volume under vacuum, the product redissolved in hexane was passed through a silica-gel column eluted by a mixture of hexane/ CH_2Cl_2 (3:1). Two bands were collected and were identified as **6** (18% yield based on **W**) and **4a** (21% yield based on **W**). Spectral data of $(\mu,\eta^1,\eta^2-CH_3CH=CH)(\mu-H)Os_3(CO)_{10}$, **6**: 1H NMR (C_6D_6) 6.79 (*dd*, $J_{H-H} = 13.7, 1.3$ Hz, =CH), 3.93 (*dq*, $J_{H-H} = 13.7, 5.8$ Hz, =CH), 1.32 (*d*, $J_{H-H} = 5.8$ Hz, CH_3), -19.12 (*d*, $J_{H-H} = 1.3$ Hz, Os-H-Os).

Isolation of $(CH_2CH=CH)_2(\mu-H)_2Os_6(CO)_{20}$ (7)

The reaction of **2a** with **3** was carried out in CH_3CN under dinitrogen for 20 min. The solution was then exposed to air overnight. The solvent was removed under vacuum and the residue extracted by hexane/ CH_2Cl_2 to give a brown solution. The solution passed a silica-gel packed column using hexane as eluent. Complex **7** was isolated in a small quantity (about 4%); thus only IR spectra were obtained. Crystals were grown from hexane. IR spectra of **7** (C_2Cl_4): 2100(*w*), 2081(*m*), 2071(*m*), 2059(*s*), 2052(*s*), 2021(*s*), 2011(*s*), 2003(*s*), 1998(*m,sh*), 1987(*w,sh*), 1975(*w*) cm^{-1} . The structure of **7** was determined by single crystal X-ray diffraction.

Reaction of $\text{Cp}(\text{CO})_2[\text{P}(\text{OMe})_3]\text{W}(\text{CH}_2\text{C}\equiv\text{CH})$ (1b**) with $\text{H}_2\text{Os}_3(\text{CO})_{10}$**

A solution of $\text{H}_2\text{Os}_3(\text{CO})_{10}$ (210 mg, 0.25 mmol) in C_6H_6 (5 mL) was added slowly at room temperature to a solution of **1b** (93 mg, 0.20 mmol) in C_6H_6 (1 mL). The solution was stirred for 1.5 h; the volume of the solvent was reduced under vacuum to cause precipitation and the solid was separated from the mixture by filtration and the solid redissolved in hexane to give a yellow solution. Recrystallization at low temperature gave $\text{Cp}(\text{CO})_2[\text{P}(\text{OMe})_3]\text{W}(\mu, \eta^1, \eta^2\text{-CH}_2\text{CH}=\text{CH})(\mu\text{-H})\text{Os}_3(\text{CO})_{10}$, **4b** (230 mg, 0.17 mmol) as a yellow-orange powder in 88% yield based on **1b**. Spectral data of **4b**: IR (C_6H_{14}): 2098(s), 2068(s), 2054(vs), 2045(s), 2014(vs), 2005(s), 1983(s), 1878(s, ν_{CO}) cm^{-1} ; ^1H NMR (C_6D_6) 6.55 (*dd*, $J_{\text{H-H}} = 14.5, 1.4$ Hz, =CH), 6.31 (*dd*, $J_{\text{H-H}} = 14.5, 8.3$ Hz, =CH), 4.54 (*d*, $J_{\text{P-H}} = 1.6$ Hz, Cp), 3.14 (*d*, $J_{\text{P-H}} = 11.6$ Hz, P(OMe)₃), 2.32 (*dd*, $J_{\text{H-H}} = 8.3, J_{\text{P-H}} = 3.2$ Hz, CH₂), -17.46 (*d*, $J_{\text{H-H}} = 1.4$ Hz, Os-H); ^{31}P NMR (C_6D_6) 156.2 (*s*, $J_{\text{P-W}} = 378.1$ Hz, P(OMe)₃); Anal. Calcd for $\text{C}_{23}\text{H}_{19}\text{O}_{15}\text{Os}_3\text{PW}$: C, 20.91; H, 1.45. Found: C, 21.22, H, 1.57. When the reaction was carried out in an NMR tube, a triosmium cluster **6** and **4b** was observed in the NMR spectrum. The amount of complex **6** increases with increase of **3** used.

Reaction of $\text{Cp}(\text{CO})_2[\text{P}(\text{OMe})_3]\text{W}(\text{CH}=\text{C}=\text{CH}_2)$ (2b**) with $\text{H}_2\text{Os}_3(\text{CO})_{10}$**

A solution of $\text{H}_2\text{Os}_3(\text{CO})_{10}$ (40 mg, 0.047 mmol) in C_6D_6 (0.5 mL) was added at room temperature to a solution of **2b** (19 mg, 0.040 mmol) in C_6D_6 (0.5 mL) to give a dark brown solution. The reaction was monitored by NMR spectroscopy. A complex observed in about 50% NMR yield was identified as $\text{Cp}(\text{CO})_2[\text{P}(\text{OMe})_3]\text{W}(\text{CH}_2\text{CH}=\text{CH}_2)$ (**5b**) by comparison with the authentic sample described below. We were unable to identify other products.

Synthesis of $\text{Cp}(\text{CO})_2[\text{P}(\text{OMe})_3]\text{W}(\text{CH}_2\text{CH}=\text{CH}_2)$ (5b**)**

A solution of $\text{Cp}(\text{CO})_2[\text{P}(\text{OMe})_3]\text{W}$ (1.04 mmol) in THF (5 mL), prepared from the reaction of $\{\text{Cp}(\text{CO})_2[\text{P}(\text{OMe})_3]\text{W}\}_2$ (0.51 g, 0.52 mmol) with excess Na/Hg followed by decanting the solution and centrifugation to remove solid residue, was added slowly at -20°C to a solution of allyl bromide (0.14 g, 1.16 mmol) in THF (1 mL). The solution was stirred for 1 h; the solvent was removed under vacuum and the product was extracted into hexane to give a yellow solution. Removal of the solvent under vacuum gave **5b** (259 mg, 0.55 mmol) as an orange powder in 53% yield based on W. Spectral data of **5b**: IR ($n\text{-C}_6\text{H}_{14}$) 1939(s), 1862(vs, ν_{CO}); 1606(m, $\nu_{\text{C=C}}$) cm^{-1} ; ^1H

NMR (C_6D_6) 6.55 (*m*, $J_{\text{H-H}} = 16.6, 9.7, 8.4$ Hz, =CH), 4.93 (*m*, $J_{\text{H-H}} = 16.6, 2.5, 1.2$ Hz, =CH), 4.70 (*dd*, $J_{\text{H-H}} = 9.7, 2.5$ Hz, =CH), 4.63 (*d*, $J_{\text{P-H}} = 1.4$ Hz, Cp), 3.26 (*d*, $J_{\text{P-H}} = 11.7$ Hz, P(OMe)₃), 2.52 (*m*, $J_{\text{H-H}} = 8.4, 1.2, J_{\text{P-H}} = 4.2$ Hz, CH₂); ^{13}C NMR (C_6D_6) 226.4 (*d*, $J_{\text{P-C}} = 25.4$ Hz, CO), 147.9 (=C β), 105.2 (=C γ), 91.1 (*s*, Cp), 52.4 (*d*, $J_{\text{P-C}} = 5.5$ Hz, P(OMe)₃), -6.1 (*d*, $J_{\text{P-C}} = 9.6$ Hz, CH₂); ^{31}P NMR (C_6D_6) 164.2 (*s*, $J_{\text{P-W}} = 397.6$ Hz, P(OMe)₃). Anal. Calcd for $\text{C}_{13}\text{H}_{19}\text{O}_5\text{PW}$: C, 33.21; H, 4.07. Found: C, 33.59, H, 4.43.

X-ray analysis of **4b and **7****

Single crystals of **4b** and **7** suitable for X-ray diffraction were grown by recrystallization from hexane. The diffraction data were collected on a Enraf-Nonius CAD4 diffractometer equipped with graphite monochromated Mo $K\alpha$ ($\lambda_\alpha = 0.71037 \text{ \AA}$) radiation. The raw intensity data were converted to structure factor amplitudes and their E.S.D.s after correction for scan speed, background, Lorentz and polarization effects. An empirical absorption correction, based on the azimuthal scan data, was applied to the data. Crystallographic computations were carried out on a Microvax III computer using the NRCC-SDP-VAX structure determination package.¹²

A suitable single crystal of **4b** was mounted on the top of a glass fiber with glue. Initial lattice parameters were determined from 25 accurately centered reflections with 2θ values in the range $19.02\text{-}26.24^\circ$. Cell parameters and other pertinent data are collected in Table 1. Data were collected using the $\omega\text{-}2\theta$ scan method. The final scan speed for each reflection was determined from the net intensity gathered during an initial prescan and was in the range $2\text{-}7^\circ \text{ min}^{-1}$. The ω scan angle was determined for each reflection according to the equation $A + B\text{tan}\theta$ for which A and B were set at values 0.75 and 0.35, respectively. Three test reflections were measured every 30 min throughout the 22.3 h of data collection and showed no apparent decay. Merging equivalent and duplicate reflections gave a total of 4117 unique data of which 2744 were considered observed, $I > 2\sigma(I)$. The structure was first solved by using the heavy atom method (Patterson synthesis) which revealed the positions of metal atoms. The remaining atoms were found in a series of alternating difference Fourier maps and least-squares refinements. The quantity minimized by the least squares program was $w(|F_o| - |F_c|)^2$, in which w is the weight of a given operation. The analytical forms of the scattering factor tables for the neutral atoms were used.¹³ The non-hydrogenic atoms were refined anisotropically. Hydrogen atoms were included in the structure factor calculations in their expected positions on the basis of idealized bonding geometry but were not refined in least

squares. All hydrogens were assigned isotropic thermal parameters $1-2 \text{ \AA}^2$ larger than the equivalent B_{iso} of the atom to which they were bonded. The final residuals of this refinement were $R = 0.057$ and $R_w = 0.064$.

The procedures for the preparation of **7** were similar to those for **4b**. The unit cell parameters were also determined from 25 accurately centered reflections. Cell parameters and other pertinent data are collected in Table 1. The final scan speed was in the range $2-7^\circ \text{ min}^{-1}$. The ω scan angle was determined for each reflection according to the equation $A + B \tan \theta$ for which A and B were set at values 0.7 and 0.35, respectively. The structure was first solved by using the heavy-atom method (Patterson synthesis) which led to the location of the metallic atom positions. The remaining atoms were found in a series of alternating difference Fourier maps and least-squares refinements. The final residuals of this refinement were $R = 0.054$ and $R_w = 0.048$.

RESULTS AND DISCUSSION

Reactions of Tungsten Propargyl and Allenyl Complexes with $\text{H}_2\text{Os}_3(\text{CO})_{10}$

The reactions of **1a** and **2a** with **3** are summarized in Chart I. The triosmium cluster $\text{H}_2\text{Os}_3(\text{CO})_{10}$ (**3**) with a formal Os=Os double bond, reacts readily with unsaturated molecules. For instance, the reaction of propyne with **3** afforded $(\mu, \eta^1, \eta^2\text{-CH}_3\text{CH}=\text{CH})(\mu\text{-H})\text{Os}_3(\text{CO})_{10}\text{H}$ (**6**) in high yield.¹⁴ We carried out the reaction of $\text{Cp}(\text{CO})_3\text{WCH}_2\text{C}\equiv\text{CH}$ (**1a**) with **3** at room temperature in

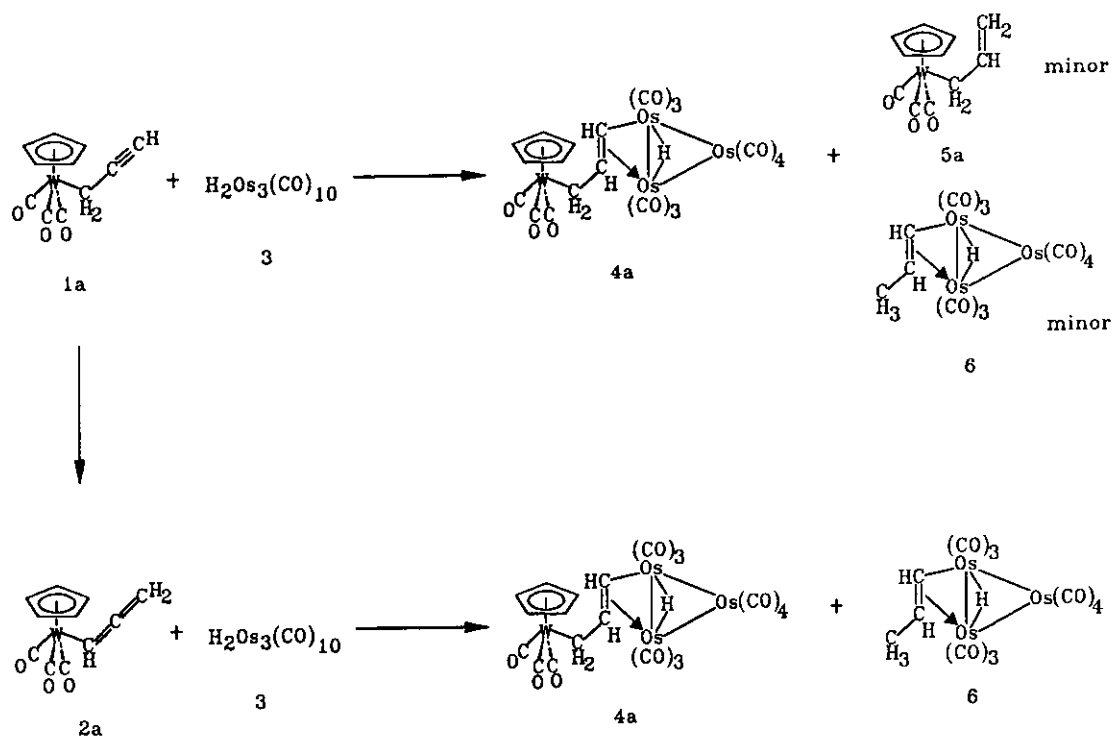
benzene. Addition of the hydride ligand of **3** to the $\text{C}\equiv\text{C}$ triple bond of the propargyl group occurred as expected and a tetranuclear complex $\text{Cp}(\text{CO})_3\text{W}(\mu, \eta^1, \eta^2\text{-CH}_2\text{CH}=\text{CH})\text{Os}_3(\text{CO})_{10}\text{H}$ (**4a**) was isolated in moderate yield. Complex **4a** was identified mostly by ^1H NMR. The coupling parameter 15.6 Hz of two olefinic protons falls in the range of trans-coupling. The upfield doublet resonance at $\delta -17.46$ with H-H coupling parameter of 1.4 Hz is assigned to the hydride ligand on the osmium cluster. With excess **3**, a η^1 -allylic complex $\text{Cp}(\text{CO})_3\text{WCH}_2\text{CH}=\text{CH}_2$ (**5a**) and $(\mu, \eta^1, \eta^2\text{-CH}_3\text{CH}=\text{CH})(\mu\text{-H})\text{Os}_3(\text{CO})_{10}$ (**6**) were observed in the NMR spectrum.

Treatment of the tungsten allenyl complex $\text{Cp}(\text{CO})_3\text{WCH}=\text{C}=\text{CH}_2$ (**2a**) with **3** in benzene resulted in a mixture of compounds which can be observed only in the NMR spectrum (see experimental section). These initial products were not isolated. When the reaction mixture, separated from the solvent, was passed through a silica-gel packed column, a mixture with 1:1 ratio of **4a** and **6** was obtained. Formation of **4a** in the reaction can be envisaged as tungsten migration of **2a** back to **1a** followed by the addition of Os-H to the unsaturated ligand. Transformation of **1a** to **2a** is known to proceed by tungsten migration, even though the transformation of propargyl and allenyl ligands is unidirectional, namely from propargyl complex to allenyl complex (no propargyl complex was detected in a solution of allenyl complex by a spectral method). As a result of the small activation energy³ of this process, one cannot rule out the reverse transformation. Addition of Os-H to the propargyl ligand of **1a** resulted in formation of **4a**; further hydride addition gave **5a**. As was mentioned in the intro-

Table 1. Crystal and Intensity Collection Data for $\text{Cp}(\text{CO})_2[\text{P}(\text{OMe})_3]\text{W}(\eta^1, \eta^2\text{-CH}_2\text{CH}=\text{CH})\text{Os}_3(\text{CO})_{10}\text{H}$, **4b** and $\text{H}_2\text{Os}_6(\text{CO})_{20}(\text{C}_6\text{H}_8)$, **7**

Molecular formula	$\text{C}_{23}\text{H}_{19}\text{O}_{15}\text{Os}_3\text{PW}$, 4b	$\text{C}_{26}\text{H}_{10}\text{O}_{20}\text{Os}_6$, 7
Molecular weight	1319.80	1783.52
Space group	$\text{P}\bar{1}$	$\text{P}2_1/\text{c}$
$a/\text{\AA}$	9.490(4)	14.448(7)
$b/\text{\AA}$	13.072(7)	13.689(4)
$c/\text{\AA}$	13.770(9)	19.224(4)
α°	91.89(5)	90.00
β°	106.71(5)	107.14(2)
γ°	104.07(4)	90.00
$V/\text{\AA}^3$	1577.3(15)	3363.1(5)
Z	2	4
Crystal dimension, /mm ³	0.05x0.3x0.3	0.4x0.4x0.5
Radiation	Mo $K\alpha$ $\lambda = 0.7107 \text{ \AA}$	
2θ range	$2^\circ\text{-}45^\circ$	$2^\circ\text{-}45^\circ$
Scan type	$2\theta/\omega$	
Total number of reflections	4117	4917
unique reflections $I > 2\sigma(I)$	2744	2860
R	0.057	0.054
R_w	0.064	0.048

Chart I



duction, in the reactions of amine with the propargyl/allenyl complex system, there is regio-specificity in C-C bond formation. However, in the reactions of osmium hydride with the same system, no specific reaction pattern between propargyl and allenyl ligands was identified. The fact that **5a** was not observed in the reaction of **2a** with **3** may indicate that **5a** can be obtained only from the hydrogenation of the $\text{C}\equiv\text{C}$ triple bond of **1a**, but not from that of $\text{C}_\alpha=\text{C}_\beta$ of **2a**.

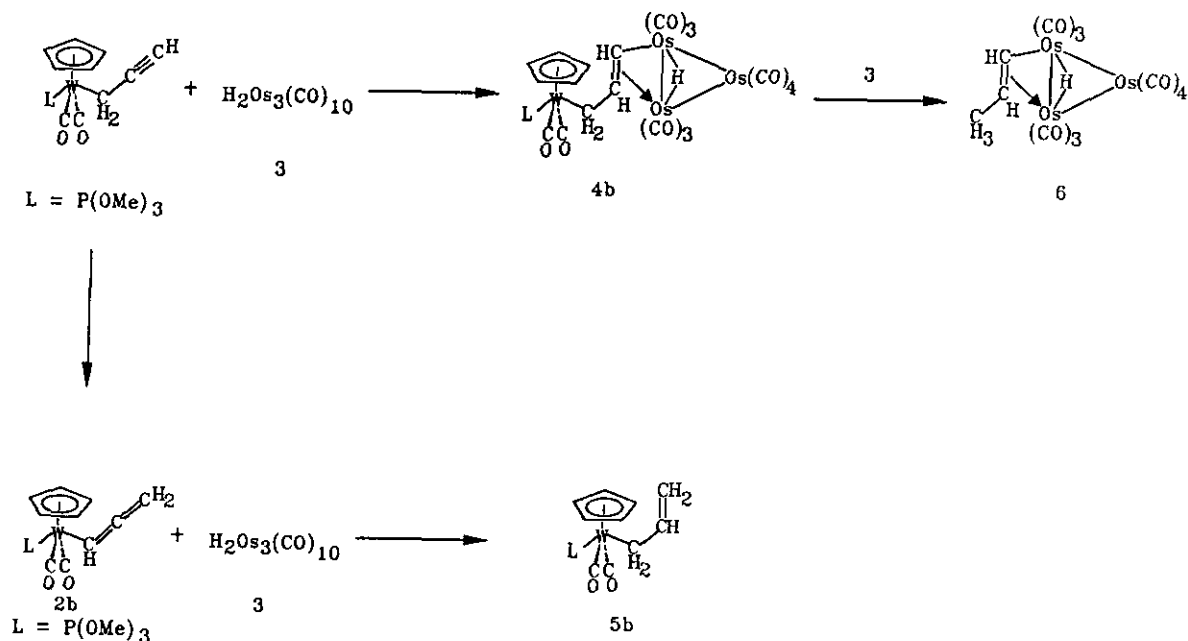
When the reaction of **2a** with **3** was carried out in CH_3CN followed by exposure of the mixture to air, a C-C coupling product $(\text{CH}_2\text{CH}=\text{CH})_2(\mu\text{-H})_2\text{Os}_6(\text{CO})_{20}$ (**7**) was obtained in about 4% yield after passing the mixture through a silical gel packed column. The structure of complex **7** was determined by single crystal X-ray diffraction. Two allenyl ligands coupled intermolecularly to form a hexa-1,5-diene ligand with two double bonds bound to two triosmium clusters in a μ,η^2 -fashion. A new C-C bond replaced the ruptured W-C bond. Coupling of two allenyl ligands may proceed possibly through a complicated radical mechanism. Intentional exposure of **4a** to air failed to produce **7** in significant quantity.

Reactions of Substituted Tungsten Propargyl and Allenyl Complexes with $\text{H}_2\text{Os}_3(\text{CO})_{10}$

The reactions of **1b** and **2b** with **3** are summarized in Chart II. The reaction of the substituted propargyl complex **1b** with $\text{H}_2\text{Os}_3(\text{CO})_{10}$ was carried out in benzene to afford cleanly a yellow-orange compound **4b**. The ^1H NMR spectrum of **4b** reveals a doublet at δ 4.54 ppm with $J_{\text{P-H}} = 1.5$ Hz that is assigned to a $\eta^5\text{-C}_5\text{H}_5$ group; two multiplets were observed in δ 6.55 and 6.31, in ranges characteristic of protons of coordinated olefins. These spectral results are in accord with **4b** being a tetranuclear complex $\text{Cp}(\text{CO})_2[\text{P}(\text{OMe})_3]\text{W}(\mu,\eta^1,\eta^2\text{-CH}_2\text{CH}=\text{CH})(\mu\text{-H})\text{Os}_3(\text{CO})_{10}$. Complex **4b** is envisaged to result from addition of the Os-H group to the $\text{C}\equiv\text{C}$ triple bond of the propargyl group. When complex **3** was used in excess in the reaction, along with the formation of **4b**, the triosmium complex **6** was also isolated from the reaction, but no **5b** was observed. Excess hydride caused the cleavage of the W-C bond and resulted in the transfer of a C_3 unit to the triosmium cluster, in contrast to what was observed in the reaction of **3** with non-substituted complex **2a**.

Reaction of the monophosphite-substituted tungsten

Chart II



allenyl complexes **2b** with **3** gave only the monophosphite-substituted allylic tungsten complex Cp(CO)₂[P(OMe)₃]W(CH₂CH=CH₂) (**5b**). The authentic complex **5b** is prepared from the reaction of Cp(CO)₂[P(OMe)₃]W with allyl bromide. Formation of **5b** in the reaction of **2b** and **3** indicates that hydrogenation takes place selectively at the C_α=C_β double bond of the allenyl ligand which was not observed in the reaction of **2a** with **3**. The fact that no **4b** was detected in the reaction of **2b** with **3** monitored by NMR indicates that tungsten migration in **2b** back to **1b** may be either slow or nonexistent. The phosphite ligand

here plays an important role¹⁵ to guide the reaction pathway; it both prevents back transposition of the allenyl ligand to the propargyl ligand and controls the M-C bond cleavage. The M-C(sp²) single bond, e.g. in the metal aryl complex, is more stable than the corresponding M-C(sp³) bond (in the metal alkyl complex).¹⁶ In the reaction of **2b** (containing a M-C(sp²) bond) with **3**, the W-C bond remains intact whereas the same chemical bond in **1b** was cleaved in the presence of hydride.

Molecular and Crystal Structures of **4b** and **7**

ORTEP¹⁷ drawings of **4b** and **7** are shown in Figs. 1

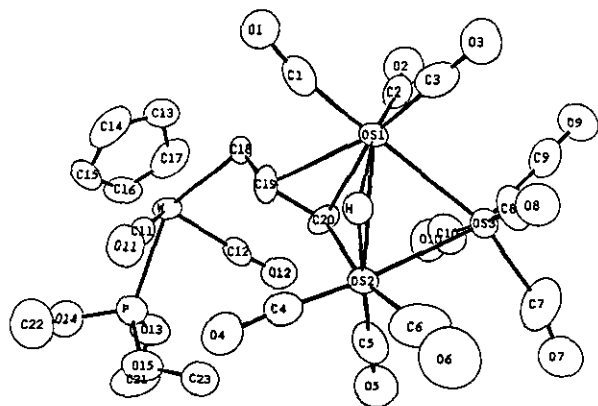


Fig. 1. ORTEP drawing of complex **4b**.

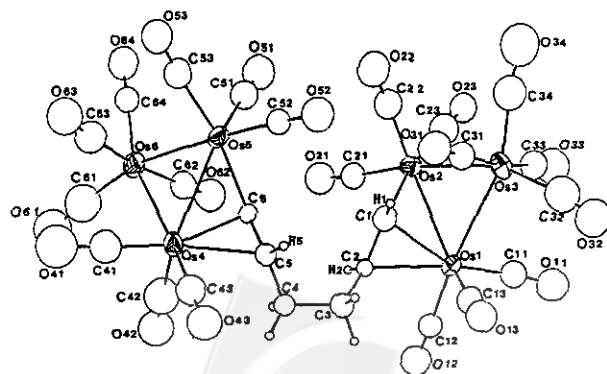


Fig. 2. ORTEP drawing of complex **7**.

Table 2. Atomic Parameters x,y,z and Biso. of Cp(CO)₂[P(OMe)₃]W(μ,η^1,η^3 -C₃H₄)Os₃(CO)₁₀H
E.S.Ds. Refer to the Last Digit Printed

	x	y	z	Biso Å
Os1	0.87973(14)	0.17087(12)	0.34286(10)	2.64(7)
Os2	0.64002(14)	0.27166(12)	0.30068(11)	3.07(7)
Os3	0.58834(15)	0.06746(12)	0.19613(11)	3.04(8)
W	1.16622(14)	0.57917(12)	0.24912(11)	2.79(7)
P	1.0368(10)	0.7144(8)	0.1963(7)	3.8(5)
C1	1.062(4)	0.239(3)	0.455(3)	4.1(21)
C2	0.971(3)	0.114(3)	0.2537(22)	2.9(18)
C3	0.850(3)	0.046(3)	0.403(3)	4.8(23)
C4	0.687(3)	0.394(3)	0.373(3)	4.2(22)
C5	0.547(4)	0.311(3)	0.185(3)	4.9(23)
C6	0.463(4)	0.208(4)	0.347(3)	8.1(34)
C7	0.375(4)	0.036(4)	0.120(3)	6.9(27)
C8	0.539(4)	0.017(3)	0.309(3)	4.4(22)
C9	0.625(3)	-0.065(3)	0.1589(24)	3.9(19)
C10	0.660(4)	0.134(3)	0.098(3)	5.3(26)
C11	1.093(3)	0.599(3)	0.3616(22)	2.8(17)
C12	0.990(4)	0.500(3)	0.1362(23)	3.6(20)
C13	1.404(4)	0.538(3)	0.258(3)	5.1(24)
C14	1.424(4)	0.623(4)	0.331(3)	7.3(30)
C15	1.397(4)	0.710(3)	0.284(3)	5.4(25)
C16	1.351(4)	0.680(3)	0.185(3)	5.1(24)
C17	1.343(4)	0.576(4)	0.161(3)	6.7(29)
C18	1.123(3)	0.4032(25)	0.2922(22)	2.5(16)
C19	0.985(3)	0.372(3)	0.3163(22)	3.5(18)
C20	0.844(3)	0.309(3)	0.2469(24)	3.4(18)
C21	0.945(4)	0.805(4)	0.031(3)	9.2(35)
C22	1.119(5)	0.856(4)	0.332(4)	8.8(35)
C23	0.752(4)	0.615(3)	0.202(3)	5.6(25)
O1	1.1737(23)	0.2657(21)	0.5240(18)	5.1(15)
O2	1.0384(24)	0.0890(22)	0.2046(17)	5.3(16)
O3	0.827(3)	-0.0345(22)	0.4374(20)	6.0(16)
O4	0.7123(24)	0.4854(22)	0.4283(18)	5.3(15)
O5	0.473(3)	0.3402(24)	0.1062(20)	6.9(18)
O6	0.364(3)	0.183(3)	0.377(3)	9.9(27)
O7	0.259(3)	0.0406(23)	0.0691(19)	6.3(17)
O8	0.4925(23)	-0.0136(20)	0.3759(17)	4.7(15)
O9	0.647(3)	-0.1398(21)	0.1374(19)	5.7(16)
O10	0.699(3)	0.1691(24)	0.0322(19)	6.4(17)
O11	1.0485(25)	0.6095(21)	0.4288(17)	5.1(16)
O12	0.8946(24)	0.4500(22)	0.0658(18)	5.5(16)
O13	1.012(3)	0.7288(22)	0.0820(18)	5.7(17)
O14	1.1237(24)	0.8309(21)	0.2419(19)	5.3(16)
O15	0.879(3)	0.7103(22)	0.2163(19)	5.8(17)
H	0.723	0.224	0.441	2.7

Biso is the Mean of the Principal Axes of the Thermal Ellipsoid.

and 2 respectively. Final atomic positional parameters, selective interatomic bond distances and bond angles are listed in Tables 2-7. The crystals of these compounds are built of discrete molecules which show no unusual intermolecular distances. Complex 4b consists of a closed triangular cluster of three osmium atoms with ten linear terminal carbonyl ligands and a tungsten unit bridged by a C₃ group. Complex 7 contains two closed triangular clusters

Table 3. Bond Distances/Å of Cp(CO)₂[P(OMe)₃]W(μ,η^1,η^3 -C₃H₄)Os₃(CO)₁₀H

Os(1)-Os(2)	2.828(2)	W-C(18)	2.36(3)
Os(1)-Os(3)	2.889(3)	P-O(13)	1.55(2)
Os(1)-C(1)	1.95(4)	P-O(14)	1.56(3)
Os(1)-C(2)	1.92(3)	P-O(15)	1.59(2)
Os(1)-C(3)	1.85(4)	C(1)-O(1)	1.17(4)
Os(1)-C(19)	2.65(3)	C(2)-O(2)	1.14(3)
Os(1)-C(20)	2.31(3)	C(3)-O(3)	1.17(5)
Os(1)-H	2.47	C(4)-O(4)	1.32(5)
Os(2)-Os(3)	2.853(3)	C(5)-O(5)	1.24(4)
Os(2)-C(4)	1.75(4)	C(6)-O(6)	1.12(4)
Os(2)-C(5)	1.74(4)	C(7)-O(7)	1.14(4)
Os(2)-C(6)	1.97(4)	C(8)-O(8)	1.18(4)
Os(2)-C(20)	2.22(2)	C(9)-O(9)	1.09(4)
Os(2)-H	2.04	C(10)-O(10)	1.14(4)
Os(3)-C(7)	1.93(4)	C(11)-O(11)	1.14(3)
Os(3)-C(8)	1.84(3)	C(12)-O(12)	1.17(4)
Os(3)-C(9)	1.93(4)	C(13)-C(14)	1.40(6)
Os(3)-C(10)	1.83(3)	C(13)-C(17)	1.44(5)
W-P	2.405(9)	C(14)-C(15)	1.38(6)
W-C(11)	1.90(3)	C(15)-C(16)	1.32(6)
W-C(12)	1.96(3)	C(16)-C(17)	1.36(6)
W-C(13)	2.41(3)	C(18)-C(19)	1.41(4)
W-C(14)	2.29(3)	C(19)-C(20)	1.44(4)
W-C(15)	2.34(3)	C(21)-O(13)	1.41(5)
W-C(16)	2.33(3)	C(22)-O(14)	1.29(5)
W-C(17)	2.34(3)	C(23)-O(15)	1.47(5)

of three osmium atoms connected by a η^2,η^2 -C₆H₈ group. The η^2,η^2 -hexadiene group is derived from the coupling of two allenyl ligands.

The Os-Os bonding distances in 4b are Os(1)-Os(2) = 2.828 (2), Os(1)-Os(3) = 2.889 (3) and Os(2)-Os(3) = 2.853 (3) Å. The corresponding Os-Os distances found in 7 are Os(1)-Os(2) = 2.835 (2), Os(1)-Os(3) = 2.898 (2), Os(2)-Os(3) = 2.839 (2), Os(4)-Os(5) = 2.834 (2), Os(4)-Os(6) = 2.900 (2), and Os(5)-Os(6) = 2.844 (2). In 4b, the hydride ligand which bridges the smallest Os-Os distance, was located but not refined crystallographically, Os(2)-H = 2.04 and Os(1)-H = 2.47 Å. The same edge of the triangular Os₃ core is also bridged by a μ,η^2 -olefin ligand. The α , ω carbons of the hexadiene ligand of 7 are each bound to one Os atom in a σ -bonding fashion; and the double bond is π -bound to the other osmium metal centers. In 4b, the Os(1)-C(20), Os(2)-C(20) and Os(1)-C(19) distances of 2.31(3), 2.22(2) and 2.65(3) respectively and the C(19)-C(20) separation of 1.44 (4) plus a Os(2)-C(20)-C(19) angle of 118.0 (21)° are typical of parameters found in substituted olefins of Os cluster.¹⁴ In complex 7, two sets of hydrogen bridged Os atoms attain an 18-electron configuration by each coordinating to μ,η^2 -unsaturated groups of the newly formed hexa-1,5-diene. The length of the two double bonds in the hexadiene of 7 are 1.33 (4) and 1.37 (4)

Å. In contrast, the coordination of the carbon atom in 4a produces a significant increase (ca. 0.1 Å) of the olefinic carbon-carbon distance, 1.44 (4) Å which may be due to the

Table 4. Bond Angles/deg of $\text{Cp}(\text{CO})_2[\text{P}(\text{OMe})_3]\text{W}(\mu, \eta^1, \eta^3\text{-C}_3\text{H}_4)\text{Os}_3(\text{CO})_{10}\text{H}$

Os(2)-Os(1)-Os(3)	59.88(6)	Os(1)-Os(3)-Os(2)	59.00(7)
Os(2)-Os(1)-C(1)	116.7(9)	Os(1)-Os(3)-C(7)	160.4(13)
Os(2)-Os(1)-C(2)	130.9(9)	Os(1)-Os(3)-C(8)	83.9(11)
Os(2)-Os(1)-C(3)	116.9(8)	Os(1)-Os(3)-C(9)	100.5(9)
Os(2)-Os(1)-C(19)	70.2(6)	Os(1)-Os(3)-C(10)	87.9(12)
Os(2)-Os(1)-C(20)	49.9(6)	Os(2)-Os(3)-C(7)	101.9(13)
Os(2)-Os(1)-H	44	Os(2)-Os(3)-C(8)	84.6(11)
Os(3)-Os(1)-C(1)	172.6(9)	Os(2)-Os(3)-C(9)	159.4(9)
Os(3)-Os(1)-C(2)	87.0(9)	Os(2)-Os(3)-C(10)	88.4(13)
Os(3)-Os(1)-C(3)	84.0(11)	C(7)-Os(3)-C(8)	90.5(16)
Os(3)-Os(1)-C(19)	113.3(7)	C(7)-Os(3)-C(9)	98.4(16)
Os(3)-Os(1)-C(20)	80.6(8)	C(7)-Os(3)-C(10)	96.2(17)
Os(3)-Os(1)-H	84	C(8)-Os(3)-C(9)	91.7(14)
C(1)-Os(1)-C(2)	99.6(12)	C(8)-Os(3)-C(10)	171.2(17)
C(1)-Os(1)-C(3)	92.5(15)	C(9)-Os(3)-C(10)	92.9(15)
C(1)-Os(1)-C(19)	69.6(12)	P-W-C(11)	79.0(9)
C(1)-Os(1)-C(20)	102.2(13)	P-W-C(12)	78.6(9)
C(1)-Os(1)-H	89	P-W-C(18)	141.8(7)
C(2)-Os(1)-C(3)	91.6(14)	C(11)-W-C(12)	106.9(12)
C(2)-Os(1)-C(19)	95.4(12)	C(11)-W-C(18)	81.5(12)
C(2)-Os(1)-C(20)	92.8(12)	C(12)-W-C(18)	76.1(12)
C(2)-Os(1)-H	170	W-P-O(13)	112.3(10)
C(3)-Os(1)-C(19)	161.6(13)	W-P-O(14)	117.3(9)
C(3)-Os(1)-C(20)	163.7(11)	W-P-O(15)	120.5(10)
C(3)-Os(1)-H	85	O(13)-P-O(14)	98.4(15)
C(19)-Os(1)-C(20)	32.7(10)	O(13)-P-O(15)	106.3(13)
C(19)-Os(1)-H	90	O(14)-P-O(15)	99.0(14)
C(20)-Os(1)-H	87.9(7)	Os(1)-C(1)-O(1)	170(3)
Os(1)-Os(2)-Os(3)	61.13(7)	Os(1)-C(2)-O(2)	172(3)
Os(1)-Os(2)-C(4)	113.7(9)	Os(1)-C(3)-O(3)	177(3)
Os(1)-Os(2)-C(5)	128.4(10)	Os(2)-C(4)-O(4)	176.1(23)
Os(1)-Os(2)-C(6)	117.0(12)	Os(2)-C(5)-O(5)	175(3)
Os(1)-Os(2)-C(20)	52.7(8)	Os(2)-C(6)-O(6)	172(5)
Os(1)-Os(2)-H	58	Os(3)-C(7)-O(7)	164(4)
Os(3)-Os(2)-C(4)	174.6(10)	Os(3)-C(8)-O(8)	172(3)
Os(3)-Os(2)-C(5)	88.3(12)	Os(3)-C(9)-O(9)	179(3)
Os(3)-Os(2)-C(6)	86.4(15)	Os(3)-C(10)-O(10)	175(4)
Os(3)-Os(2)-C(20)	82.9(10)	W-C(11)-O(11)	179(3)
Os(3)-Os(2)-H	93	W-C(12)-O(12)	174.1(24)
C(4)-Os(2)-C(5)	96.5(16)	W-C(18)-C(19)	111.1(21)
C(4)-Os(2)-C(6)	95.1(18)	Os(1)-C(19)-C(18)	119.3(22)
C(4)-Os(2)-C(20)	95.1(13)	Os(1)-C(19)-C(20)	60.3(17)
C(4)-Os(2)-H	82	C(18)-C(19)-C(20)	124(3)
C(5)-Os(2)-C(6)	99.7(16)	Os(1)-C(20)-Os(2)	77.4(9)
C(5)-Os(2)-C(20)	85.3(13)	Os(1)-C(20)-C(19)	87.0(19)
C(5)-Os(2)-H	172	Os(2)-C(20)-C(19)	118.0(21)
C(6)-Os(2)-C(20)	168.1(17)	P-O(13)-C(21)	124(3)
C(6)-Os(2)-H	73	P-O(14)-C(22)	114(3)
C(20)-Os(2)-H	102	P-O(15)-C(23)	126.1(23)
		Os(1)-H-Os(2)	76

Table 5. Atomic Parameters x, y, z and Biso of $\text{H}_2\text{Os}_6(\text{CO})_{20}(\text{C}_6\text{H}_8)$ E.S.Ds. Refer to the Last Digit Printed

	x	y	z	Biso Å
OS1	0.27084(10)	0.77385(10)	0.05050(7)	2.37(6)
OS2	0.26792(11)	0.61790(11)	0.14690(7)	2.65(7)
OS3	0.43515(10)	0.73823(12)	0.17725(8)	3.06(7)
OS4	0.18718(11)	0.29289(11)	-0.15736(7)	2.77(7)
OS5	0.28784(10)	0.25617(11)	-0.00925(7)	2.41(6)
OS6	0.10762(11)	0.16072(12)	-0.07186(8)	3.13(7)
C1	0.2893(24)	0.610(3)	0.0425(18)	3.3(8)
C2	0.2167(20)	0.6328(22)	-0.0197(15)	1.6(6)
C3	0.2268(24)	0.623(3)	-0.0932(18)	3.2(8)
C4	0.1813(22)	0.5326(25)	-0.1332(17)	2.5(7)
C5	0.2357(22)	0.4459(25)	-0.0994(17)	2.4(7)
C6	0.2072(20)	0.3845(22)	-0.0563(15)	1.7(6)
C11	0.286(3)	0.895(3)	0.0968(19)	4.1(9)
O11	0.2954(20)	0.9754(22)	0.1183(15)	5.9(7)
C12	0.1553(24)	0.820(3)	-0.0180(18)	3.4(8)
O12	0.0867(19)	0.8451(21)	-0.0636(14)	5.5(7)
C13	0.3564(25)	0.812(3)	-0.0064(19)	3.8(8)
O13	0.4133(18)	0.8271(21)	-0.0350(14)	5.3(7)
C21	0.1513(25)	0.545(3)	0.1150(19)	3.7(9)
O21	0.0817(19)	0.5005(21)	0.0998(15)	5.6(7)
C22	0.341(3)	0.507(3)	0.1821(21)	4.5(9)
O22	0.3912(20)	0.4410(21)	0.1953(15)	5.8(7)
C23	0.250(3)	0.649(3)	0.2413(21)	5.3(10)
O23	0.2432(18)	0.6693(20)	0.2970(13)	4.9(6)
C31	0.490(3)	0.644(3)	0.1285(19)	3.8(9)
O31	0.5210(18)	0.5827(20)	0.1003(14)	5.3(7)
C32	0.526(3)	0.841(4)	0.1640(23)	6.3(12)
O32	0.5650(20)	0.9001(23)	0.1475(15)	6.6(8)
C33	0.378(3)	0.817(3)	0.2364(20)	4.4(9)
O33	0.3420(21)	0.8647(24)	0.2698(16)	7.0(8)
C34	0.501(3)	0.676(4)	0.2602(24)	6.2(11)
O34	0.5426(23)	0.644(3)	0.3171(18)	8.5(9)
C41	0.174(3)	0.187(3)	-0.2165(21)	5.1(10)
O41	0.1577(23)	0.112(3)	-0.2526(17)	8.5(10)
C42	0.065(3)	0.337(4)	-0.2046(24)	7.1(13)
O42	-0.0167(22)	0.3684(25)	-0.2349(17)	7.6(9)
C43	0.250(3)	0.354(3)	-0.2135(20)	4.3(9)
O43	0.2865(19)	0.3985(22)	-0.2509(15)	6.0(7)
C51	0.252(3)	0.264(3)	0.0819(20)	4.2(9)
O51	0.2361(19)	0.2692(22)	0.1325(14)	6.0(7)
C52	0.4021(23)	0.325(3)	0.0289(17)	2.8(7)
O52	0.4724(18)	0.3722(21)	0.0499(14)	5.2(7)
C53	0.359(3)	0.130(3)	0.0110(19)	4.0(9)
O53	0.4024(18)	0.0610(20)	0.0218(14)	5.0(6)
C61	-0.002(3)	0.121(4)	-0.141(3)	7.3(13)
O61	-0.0783(23)	0.102(3)	-0.1836(18)	8.5(9)
C62	0.0475(25)	0.269(3)	-0.0353(19)	4.2(9)
O62	0.0099(20)	0.3287(22)	-0.0118(15)	5.8(7)
C63	0.185(3)	0.061(3)	-0.0974(21)	5.0(10)
O63	0.2372(20)	-0.0006(23)	-0.1082(15)	6.3(8)
C64	0.1034(24)	0.085(3)	0.0086(19)	3.4(8)
O64	0.0948(19)	0.0423(21)	0.0565(14)	5.2(7)

Biso is the Mean of the Principal Axes of the Thermal Ellipsoid.

Table 6. Selected Bond Lengths/Å of $H_2Os_6(CO)_{20}(C_6H_8)$

Os(1)-Os(2),	2.835(2);	Os(1)-Os(3),	2.898(2);
Os(2)-Os(3),	2.839(2);	Os(4)-Os(5),	2.834(2);
Os(4)-Os(6),	2.900(2);	Os(5)-Os(6),	2.844(2);
Os(1)-C(11),	1.87(4);	Os(4)-C(41),	1.82(4);
Os(1)-C(12),	1.90(3);	Os(4)-C(42),	1.83(4);
Os(1)-C(13),	1.95(4);	Os(4)-C(43),	1.80(4);
Os(1)-C(2),	2.35(3);	Os(4)-C(6),	2.26(3);
Os(1)-C(1),	2.26(4);	Os(4)-C(5),	2.38(3);
Os(2)-C(21),	1.90(4);	Os(5)-C(51),	1.97(4);
Os(2)-C(22),	1.86(4);	Os(5)-C(52),	1.86(3);
Os(2)-C(23),	1.96(4);	Os(5)-C(53),	1.99(4);
Os(2)-C(1),	2.12(3);	Os(5)-C(6),	2.15(3);
Os(3)-C(31),	1.90(4);	Os(6)-C(61),	1.83(5);
Os(3)-C(32),	1.99(5);	Os(6)-C(62),	1.95(4);
Os(3)-C(33),	1.92(4);	Os(6)-C(63),	1.92(4);
Os(3)-C(34),	1.81(5);	Os(6)-C(64),	1.88(4);
C(11)-O(11),	1.17(5);	C(12)-O(12),	1.16(4);
C(13)-O(13),	1.14(4);	C(21)-O(21),	1.14(4);
C(22)-O(22),	1.14(5);	C(23)-O(23),	1.13(5);
C(31)-O(31),	1.15(5);	C(32)-O(32),	1.09(6);
C(33)-O(33),	1.14(5);	C(34)-O(34),	1.17(6);
C(41)-O(41),	1.22(5);	C(42)-O(42),	1.23(5);
C(43)-O(43),	1.18(5);	C(51)-O(51),	1.06(5);
C(52)-O(52),	1.17(4);	C(53)-O(53),	1.12(5);
C(61)-O(61),	1.19(6);	C(62)-O(62),	1.14(5);
C(63)-O(63),	1.19(5);	C(64)-O(64),	1.13(4);
C(1)-C(2),	1.37(4);	C(2)-C(3),	1.47(4);
C(3)-C(4),	1.50(5);	C(4)-C(5),	1.47(5);
C(5)-C(6),	1.33(4);		

Table 7. Selected Bond Angles/deg of $H_2Os_6(CO)_{20}(C_6H_8)$

Os(1)-C(11)-O(11),	173(3);	Os(1)-C(12)-O(12),	175(3);
Os(1)-C(13)-O(13),	172(3);	Os(1)-C(21)-O(21),	176(3);
Os(2)-C(22)-O(22),	169(3);	Os(1)-C(23)-O(23),	176(3);
Os(3)-C(31)-O(31),	176(3);	Os(1)-C(32)-O(32),	169(4);
Os(3)-C(33)-O(33),	178(3);	Os(1)-C(34)-O(34),	173(4);
Os(4)-C(41)-O(41),	172(4);	Os(1)-C(42)-O(42),	178(4);
Os(4)-C(43)-O(43),	175(3);	Os(1)-C(51)-O(51),	177(3);
Os(5)-C(52)-O(52),	176(3);	Os(1)-C(53)-O(53),	176(3);
Os(6)-C(61)-O(61),	173(4);	Os(1)-C(62)-O(62),	175(3);
Os(6)-C(63)-O(63),	175(3);	Os(1)-C(64)-O(64),	175(3);
C(2)-C(3)-C(4),	114(3);	C(3)-C(4)-C(5),	110(3);
C(4)-C(5)-C(6),	124(3);	Os(4)-C(6)-Os(5),	79.9(10);
Os(4)-C(6)-C(5),	78.4(19);	Os(5)-C(6)-C(5),	123.3(2);
Os(1)-C(1)-Os(2),	80.5(12);	Os(1)-C(1)-C(2),	76.3(2);
Os(2)-C(1)-C(2),	121.8(24);	C(1)-C(2)-C(3),	123(3);
C(11)-Os(1)-C(11),	89.3(15);	C(11)-Os(1)-C(13),	91.3(16);
C(12)-Os(1)-C(13),	95.4(15);	C(1)-Os(1)-C(11),	155.9(14);
C(1)-Os(1)-C(12),	112.3(14);	C(1)-Os(1)-C(13),	96.9(14);
C(21)-Os(2)-C(22),	92.4(16);	C(21)-Os(2)-C(23),	93.8(16);
C(22)-Os(2)-C(23),	93.4(17);	C(1)-Os(2)-C(21),	91.9(14);
C(1)-Os(2)-C(22),	94.6(15);	C(1)-Os(2)-C(23),	170.0(16);
C(31)-Os(3)-C(32),	91.8(17);	C(31)-Os(3)-C(33),	170.9(16);
C(31)-Os(3)-C(34),	85.7(18);	C(32)-Os(3)-C(33),	95.5(18);
C(32)-Os(3)-C(34),	104.4(19);	C(33)-Os(3)-C(34),	87.1(19);
C(41)-Os(4)-C(42),	92.6(20);	C(41)-Os(4)-C(43),	88.4(18);
C(42)-Os(4)-C(43),	97.6(19);	C(6)-Os(4)-C(41),	160.8(15);
C(6)-Os(4)-C(42),	90.6(17);	C(6)-Os(4)-C(43),	107.3(14);
C(51)-Os(5)-C(52),	93.2(15);	C(51)-Os(5)-C(53),	97.5(16);
C(52)-Os(5)-C(53),	91.2(15);	C(6)-Os(5)-C(51),	94.3(14);
C(6)-Os(5)-C(52),	93.4(13);	C(6)-Os(5)-C(53),	167.1(13);
C(61)-Os(6)-C(62),	96.1(19);	C(61)-Os(6)-C(63),	92.6(20);
C(61)-Os(6)-C(64),	101.6(19);	C(62)-Os(6)-C(63),	171.3(15);
C(62)-Os(6)-C(64),	90.0(16);	C(63)-Os(6)-C(64),	88.7(16);

presence of the remote W metal center. The alkene protons are in a trans configuration in both cases. The hydride ligands of **7** were not located in the difference map and, based on the 18-electron rule, presumably sit between the Os metal atoms bridged by the two alkene ligands.

CONCLUSION

The reactions of the tungsten propargyl and allenyl complexes and their phosphite substituted analogues with $H_2Os_3(CO)_{10}$ have been investigated. There are reactions of three different types: (1) addition of the hydride ligand to the $C\equiv C$ bond affording a tetranuclear complex; (2) in the presence of excess osmium hydride, cleavage of the W-C bond of the tetranuclear compound, illustrating transfer of the C_3 unit from tungsten to an edge of the Os cluster; (3) hydrogenation of the $C\equiv C$ or $C=C$ bond by excess osmium hydride yielding a mononuclear tungsten complex with an η^1 -allyl ligand. Type (1) is the predominate reaction pathway. No selectivity was observed in the reactions of **3** with complexes that contain no phosphite ligand. The phosphite ligand on the tungsten metal however imparts some

selectivity in directing the reaction pathway.

ACKNOWLEDGMENT

We thank the National Science Council of the Republic of China for support of this work.

Received August 21, 1991.

Key Words

Propargyl tungsten complex; Triosmium cluster; Hydride addition.

REFERENCES

- Collman, J. P.; Hegedus, L. S.; Norton, J. R.; Finke, R. G. *Principles and Applications of Organotransition Metal*

- Chemistry*; University Science Books: Mill Valley, CA, 1987; Chapter 11.
- Henrici-Olive, G.; Olive, S. *Coordination and Catalysis*; Verlag Chemie: Weinheim, 1977; Chapter 8.
 - Keng, R. S.; Lin, Y. C. *Organometallics* 1990, 9, 289.
 - Chen, M. C.; Keng, R. S.; Lin, Y. C.; Wang, Y.; Cheng, M. C.; Lee, G. H. *J. Chem. Soc., Chem. Commun.*, 1990, 1138.
 - Tseng, T. W.; Wu, I. Y.; Lin, Y. C.; Chen, C. T.; Chen, M. C.; Tsai, Y. J.; Chen, M. C.; Wang, Y. *Organometallics* 1991, 10, 43.
 - (a) Blau, R. J.; Siriwardane, U. *Organometallic* 1991, 10, 1627. (b) Chetcuti, M. J.; Fanwick, P. E.; McDonald, S. R.; Rath, N. N. *Organometallics* 1991, 10, 1551.
 - Birdwhistell, R.; Hackett, P.; Manning, A. R. *J. Organomet. Chem.* 1978, 157, 177.
 - King, R. B.; Stone, F. G. A. *Inorg. Synth.* 1963, 7, 99.
 - Knox, S. A. R.; Koepke, J. W.; Andrews, M. A.; Kasez, H. D. *J. Am. Chem. Soc.* 1975, 97, 3942.
 - Thomasson, J. E.; Robinson, P. W.; Ross, D. A.; Wojcicki, A. *Inorg. Chem.* 1971, 10, 2130.
 - Dub, M. *Organometallic Compounds*, 2nd ed.; Springer Verlag: Berlin, 1966; Vol 1.
 - Gabe, E. J.; Lee, F. L.; LePage, Y. In *Crystallographic Computing 3*; Sheldrick, G. M.; Kruger, C.; Goddard, R. Eds.; Clarendon Press: Oxford, England, 1985; p 167.
 - International Tables for X-ray Crystallography*; D. Reidel: Dordrecht, Boston, 1974; Vol. IV.
 - (a) Deeming, A. J.; Underhill, M. *J. Chem. Soc., Dalton Trans.*, 1974, 1415. (b) Deeming, A. J.; Hasso, S.; Underhill, M. *J. Chem. Soc., Dalton Trans.*, 1975, 1614. (c) Green, M.; Orpen, A. G.; Schaverien, C. J. *J. Chem. Soc., Chem. Commun.*, 1984, 37. (d) Evans, J.; Johnson, B. F. G.; Lewis, J.; Matheson, T. W. *J. Organomet. Chem.* 1975, 97, C16.
 - (a) Barrett, A. G.; Carpenter, N. E.; Mortier, J.; Sabat, M. *Organometallics* 1990, 9, 151. (b) Stack, J. G.; Doney, J. J.; Bergman, R. G.; Heathcock, C. H. *Organometallics* 1990, 9, 453.
 - Yamamoto, A. *Organotransition Metal Chemistry*; Wiley: New York, 1985; Chapter 3.
 - Johnson, C. K. ORTEP II, Report ORNL-5138. 1976; Oak Ridge National Laboratory, Tennessee, U.S.A.

